Thermoelectric performance of Zn-substituted type-VIII clathrate $Ba_8Ga_{16}Sn_{30}$ single crystals

Baoli Du,[1,2] Yuta Saiga,[1] Kousuke Kajisa,[1] and Toshiro Takabatake[1,a)]
[1]*Department of Quantum Matter, ADSM and IAMR, Hiroshima University, Higashi-Hiroshima 739-8530, Japan*
[2]*School of Physics and Chemistry, Henan Polytechnic University, Jiaozuo 454000, China*

(Received 8 September 2011; accepted 6 December 2011; published online 5 January 2012)

We have grown single-crystalline samples of Zn-substituted type-VIII clathrate $Ba_8Ga_{16}Sn_{30}$ with *n*-type carriers by Sn-flux method. The actual compositions of the single crystals were found to be described as $Ba_8Ga_{15.8-2y}Zn_ySn_{30.2+y}$ ($y = 0 \sim 0.54$), where the charge balance is well maintained. As y goes from 0 to 0.42, the resistivity at 300 K decreases from 5.3 to 3.0 mΩ cm gradually, but the effective mass is essentially constant at $1.2 \sim 1.5m_0$, indicating intact band structure near the conduction band minima upon Zn substitution for Ga. At elevated temperatures, the ambipolar effect on the thermal conductivity becomes less pronounced upon Zn doping, and the dimensionless figure of merit ZT for $y = 0.07$ and 0.42 remains at rather high values compared with the nondoped sample. © *2012 American Institute of Physics*. [doi:10.1063/1.3673863]

I. INTRODUCTION

Thermoelectric energy conversion, by which heat is converted directly into electricity using a class of materials known as thermoelectric (TE) materials based on Seebeck effect, is of great significance for solar thermal energy conversion and industrial waste heat recovery.[1] An efficient TE material should have a high figure of merit defined as $ZT = \alpha^2 T/\rho\kappa$, where T is the absolute temperature and α, ρ, κ, are the Seebeck coefficient, electrical resistivity, and thermal conductivity of the material, all of which depend on interrelated material properties, such as electronic band structure, Fermi level, chemical composition, and atomic arrangement.[2] So, fundamental to the TE materials is the need to optimize two conflicting properties. It is the electron-crystal and phonon-glass (PGEC) concept first proposed by Slack in mid 1990s.[3]

Decoupling the thermal and electrical attributes can be achieved by designing a complex crystal structure with distinct regions providing different functions.[4] The layered oxide Na_xCoO_2 and others such as those based on the Ca–Co–O system are the well known examples of this idea.[5] The Co–O layers form metallic layers separated by insulating, disordered layers with partial occupancies. Moreover, Zintl clathrates with guest rattlers in an electron-crystal matrix may be more appropriate for substructure-based thermoelectrics due to the nature of their bonding.[6] The covalently bounded cages formed by elements in group 13 or 14 enable high carrier mobilities, whereas the local vibration (rattling) of the ionic guest atoms encapsulated in oversized cages is responsible for the ultra-low thermal conductivity by scattering the heat-carrying phonons effectively without disrupting the covalent network.[7,8]

Because of the low cost and the moderate operation temperature, Sn-based clathrates crystallized in several kinds of structure (type-I, type-III, and type-VIII) might be more competitive for serving as a basis for the design of heat-harvesting materials. For example, $Ba_8Ga_{16}Sn_{30}$ (BGS) exists in two modifications, a beta-phase crystallized in type-I clathrate,[9] and an alpha-phase with the structure of type-VIII clathrate.[10] The type-I clathrate contains two types of cages, viz., pentagonal dodecahedra and lager 14-face tetrakaidecahedra. The unit cell contains 46 atoms of the framework, which has two small and six large cavities filled by Ba atoms.[9] The type-VIII clathrate, unlike the type-I structure, has only one kind of filled cavity (E_{20+3} polyhedra), which is derived from pentagonal dodecahedra as a result of the cleavage of three E-E bonds and formation of nine new such bonds upon the addition of three E atoms.[10,11] Moreover, differential thermal analysis and annealing effect suggest that type-VIII phase is more thermodynamically stable than the type-I analog.

The electronic band structure calculation of type-VIII BGS indicated that it is an indirect gap semiconductor with a band gap of 0.32 eV. The valence band consists mainly of the bonding orbitals of Ga and Sn, while the conduction band consists of the atomic orbitals of Ba as well as those of Ga and Sn.[12] According to the Zintl concept, BGS should have the ideal composition Ba : Ga : Sn = 8 : 16 : 30. However, the real composition of the clathrate does not satisfy the Zintl rule, but a slight deviation from the stoichiometry introduces carriers in the material. In fact, type-VIII BGS crystals grown from Ga flux and Sn flux lead to *p*-type and *n*-type conduction, respectively. Fine carrier tuning by optimization of the amount of flux leads to a ZT of 1.0 and 0.9 at 450 K for *p*- and *n*-type samples.[13] By partial isoelectronic substitution of Al for the framework atom Ga, the mobility of *n*-type carriers has been enhanced while keeping the carrier density constant.[14] However, it is proved that Sb substitution for Sn in BGS creates *p*-type carriers, as opposite to the initial expectation for electron doping.[13] Furthermore, Cu-substituted single-crystalline samples $Ba_8Ga_{16-x}Cu_xSn_{30}$ ($x \leq 0.033$) exhibit

a)Author to whom correspondence should be addressed. Electronic mail: takaba@hiroshima-u.ac.jp.

largely negative Seebeck coefficient.[15] The carrier mobility at 300 K increases twice while the electron carriers density is essentially unchanged to be $3.1-4.2\times10^{19}/cm^3$, in conflict with the initial design for hole doping.

While the *ZT* of *n*-type BGS clathrates have been enhanced to 1.35 at 540 K by Cu-doping,[15] the impact mechanism of introduction of a fourth element in the system on the band structure, electrical and thermal properties are not clear yet. Now, we choose Zn in group 12 as the fourth element which is a lighter element with fewer valence electrons than both the framework atoms Ga and Sn. In analogy with the system of type-I clathrate $Ba_8Ga_{16-x}Zn_xGe_{30}$,[16] it was expected that the substitution of Ga with a lighter element Zn would appear a potent method for improving its performance. In this paper, we address the thermoelectric properties of single-crystalline samples of type-VIII clathrate $Ba_8Ga_{16-x}Zn_xSn_{30}$ at temperatures 300–600 K.

II. EXPERIMENTAL

Single crystals $Ba_8Ga_{16-x}Zn_xSn_{30}$ (BGZS) were prepared by the Sn-flux method, the details of which were described in previous papers.[17–19] High purity elements Ba (99.9%, dendritic), Ga (99.9999%, shot), Zn (99.9999%, shot), and Sn (99.999%, shot) were weighed in an atomic ratio of Ba : Ga : Zn : Sn = 8 : 16 − *x* : *x* : 50 ($0\le x\le8$) in an Ar atmosphere glovebox. The mixture was loaded in a quartz tube and then properly vacuum sealed. The tube was heated to 763 K and kept at this temperature for 20 h. In order to avoid bubbling of Zn due to the high vapor pressure, samples were heated slowly across the melting point of Zn. Then, it was slowly cooled to 663 K over 100 h and annealed for several hours. Well-shaped crystals of approximately 5 mm in diameter with a shiny metallic luster were separated from the molten Sn flux by centrifuging.

Powder x-ray diffraction (XRD) experiment was performed on ground samples using a Rigaku D/tex ultra detector and Cu K_α radiation in the 2θ range 10°–120°. The actual composition was determined by the wavelength dispersive electron-probe micro analysis (EPMA) using a JEOL JXA-8200 analyzer. The data were averaged over ten regions. The electrical resistivity ρ and Seebeck coefficient α were measured in a vacuum by the standard dc four-probe method and differential method with a home-made system and a commercial measurement system (MMR technologies), respectively. The Hall coefficient R_H was measured at room temperature by a dc method under a magnetic field of 1 T. Adopting the single-carrier model, the carrier concentration *n* and Hall mobility μ_H were calculated from the formulae $n=1/eR_H$ and $\mu_H=R_H/\rho$, where *e* is the electron charge. Thermal conductivity κ was calculated via the equation $\kappa=DC_pd$ from the thermal diffusivity *D* measured by a laser flash diffusivity method in a vacuum (LFA-502, Kyoto Electronics), specific heat C_p calculated using Dulong-Petit law, and the density *d*. All measurements were performed in the temperature range from 300 to 600 K.

III. RESULTS AND DISCUSSION

A. Composition and phase structure

Single-crystalline samples of approximately 5 mm in diameter were obtained for $Ba_8Ga_{16-x}Zn_xSn_{30}$ with $x=0.5$, 1, 2, and 5. The as-prepared samples are basically the same size with the Al-doped samples,[14] and a little smaller than the Cu-doped samples.[15] However, only less than 1/3 of the starting elements formed into single-crystalline clathrate, and the rest are mixture of polycrystalline clathrates and impurities, such as Sn and $BaGa_{4-x}Sn_x$ with the $BaNiSn_3$-type structure. The ratio of single crystal is much less than those for Al and Cu doped analogs.[14,15] In addition, holes with diameter smaller than 1 mm are always observed inside the Zn-doped single crystals. This may be a result of the high saturated vapor pressure of elemental Zn, which bubbles in the molten sample and leaves cavities in the solidified sample. For the sample with $x=8$, the maximum crystal size was 1 mm in diameter. It is noteworthy that the single crystals of all samples are stable in air and immune to moisture. However, the mixture of polycrystalline clathrates and impurities are oxidized slowly at room temperature and transformed into powder with ash color.

The crystal compositions were determined on the assumption that the total number of framework atoms is equal to 46. As is shown in Table I, the actual concentration of Zn is much less than the initial composition but roughly proportional to it. While the amount of Zn increases from 0.07 to 0.54, the content of Ga decreases from 15.7 to 14.7, reducing approximately twice the amount of Zn. No apparent change of Ba content was observed in all samples. Thus, the actual composition of the single crystal can be described as $Ba_8Ga_{15.8-2y}Zn_ySn_{30.2+y}$. In this way, the charge balance would be well maintained in crystals. This is very similar to the formula of Sb-doped samples, whose composition is written as $Ba_8Ga_{16+x}Sn_{30-x-y}Sb_y$ ($x\approx y<0.9$).[13] According

TABLE I. Atomic compositions and room-temperature properties of *n*-type $Ba_8Ga_{16-x}Zn_xSn_{30}$ samples prepared by the Sn flux method.

Nominal composition	Crystal composition				Lattice parameter (Å)	R_H (cm^3/C)	*n* ($10^{19}/cm^3$)	ρ (mΩcm)	μ_H (cm^2/Vs)	α ($\mu V/K$)	m^*/m_0
	Ba	Ga	Zn	Sn							
$x=0$	7.96	15.9	0	30.1	11.5966(1)	−0.146	4.3	5.28	27.8	−242	1.5
$x=0.5$	8.03	15.7	0.07	30.3	11.5974(2)	−0.188	3.3	4.56	41.4	−220	1.2
$x=1$	8.02	15.7	0.10	30.3	11.5997(8)	−0.104	6.0	3.50	29.7	−191	1.5
$x=2$	8.02	15.4	0.23	30.4	11.5994(2)	−0.136	4.6	3.58	38.0	−188	1.2
$x=5$	7.97	14.9	0.42	30.7	11.6041(6)	−0.104	6.0	3.00	34.8	−186	1.5
$x=8$	7.93	14.7	0.54	30.7	11.6074(1)	—	—	—	—	—	—

to the Zintl concept, the Ba atoms in the cages donate two electrons and the group 13 element Ga on the framework accommodates the electrons as lone pair and forms the clathrate structure. Due to the charge-balance constraint, the difficulty level of introducing a foreign element can be evaluated by the distance from group 13 or 14 element in the periodic table of the elements. In fact, the composition analysis of Al, Zn, Sb, and Cu in BGS agree to this conjecture very well.[13–15]

Figure 1 shows the power XRD pattern for selected samples. All patterns are assigned to the type-VIII clathrate structure with the space group $I\bar{4}3m$ except three weak peaks at $2\theta = 30.6°$, 32.0°, and 44.9° which are indexed to Sn impurity. The inset to Fig. 1 displays the y dependence of the lattice parameter of the $Ba_8Ga_{15.8-2y}Zn_ySn_{30.2+y}$ ($y = 0 \sim 0.54$) samples calculated by Rietveld refinement. Despite a little smaller covalent radius of Zn than that of Ga, the lattice parameter increases linearly with y. For type–VIII BGS, the structural refinement of single crystal XRD indicated that Ga atoms preferentially occupy the 8c site with relatively short bond length with the neighbors, while Sn atoms preferentially occupy the 12d, 2a, and 24g sites of the framework.[10] Therefore, we conjecture that the incorporated Zn atoms preferentially occupy the 8c site. In $Ba_8Ga_{15.8-2y}Zn_ySn_{30.2+y}$, extra Sn atoms of same number y with that of Zn atoms have to occupy the 8c position in the framework so that the lattice parameter should increase as observed.

B. Electrical transport properties

Figure 2(a) shows the temperature dependence of the electrical resistivity $\rho(T)$ for the samples $Ba_8Ga_{15.8-2y}Zn_ySn_{30.2+y}$ ($y = 0 \sim 0.42$). We could not collect reliable data for the sample with $y = 0.54$ because of the small size of crystals. Zn-doped samples have rather low ρ with a typical behavior of degenerate semiconductor, i.e., $\rho(T)$ increases linearly with increasing T in the whole temperature range. As y goes from 0 to 0.42, $\rho(T = 300\,\mathrm{K})$ gradually decreases from 5.3 to 3.0 mΩ cm. To gain more insight into the electrical transport behavior, the data of Hall coefficient R_H ($T = 300\,\mathrm{K}$) are presented in Table I. All samples exhibit negative values which indicate that electron is the majority charge carrier. The carrier concentration n does not change systematically with y while the values of samples with $y = 0.10$ and 0.42 are roughly 50% higher than that for $y = 0$. Such a trend of electron carrier density suggests that the extra holes introduced by the Zn substitution for Ga are compensated with the increase of the Sn atoms in the cage. This result is quiet similar with Cu-doped BGS even though the doping concentration of Zn is dozens of times larger than that of Cu.[15] Combined with the actual Sn composition in Zn-doped samples, we conclude that the electron carrier density is largely determined by the ratio of Ga and Sn. Moreover, the mobility for all Zn-doped samples increases more or less compared with the sample with $y = 0$. Both the increase of carrier density and the enhanced mobility have led to the decrease in the resistivity.

To understand the effect of Zn substitution on the electronic band structure, we calculated the effective mass m^* using the measured Seebeck coefficient α and carrier

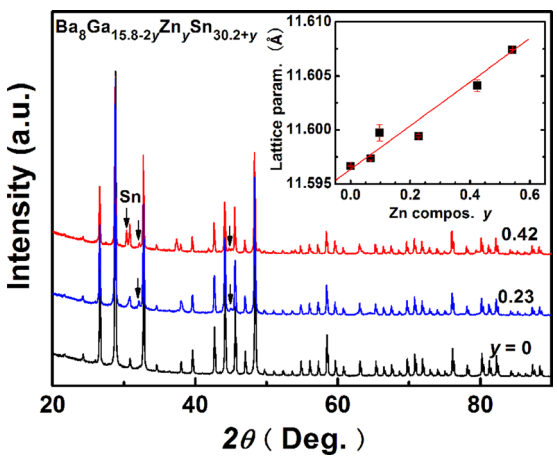

FIG. 1. (Color online) Powder x-ray diffraction patterns for $Ba_8Ga_{15.8-2y}Zn_ySn_{30.2+y}$ ($y = 0$, 0.23, and 0.42). The inset shows the lattice parameter as a function of Zn composition y ($y = 0 \sim 0.54$).

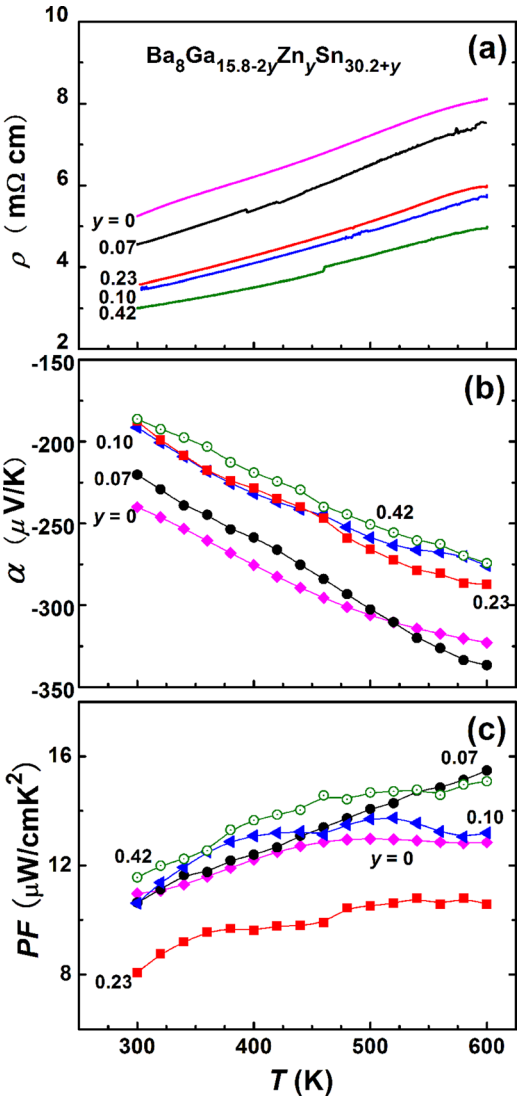

FIG. 2. (Color online) (a) Electrical resistivity ρ, (b) Seebeck coefficient α, and (c) power factor PF as a function of temperature for $Ba_8Ga_{15.8-2y}Zn_ySn_{30.2+y}$ ($y = 0 \sim 0.42$).

concentration n. Assuming a single parabolic band structure and energy-independent scattering distance, the α for a degenerate semiconductor is given by[4,20]

$$|\alpha| = \frac{8\pi^2 k_B^2}{3eh^2} m^* T \left(\frac{\pi}{3n}\right)^{2/3}, \quad (1)$$

where h is the Planck's constant and k_B is the Boltzmann's constant. The calculated values of m^* are listed in Table I, where m^* is essentially constant at $1.2 \sim 1.5 m_0$. This indicates that the band structure near the conduction band minima keeps intact upon Zn substitution of Ga.

Figure 2(b) gives the $\alpha(T)$ of the samples $Ba_8Ga_{15.8-2y}Zn_ySn_{30.2+y}$ ($y = 0 \sim 0.42$) as a function of temperature. For all specimens, α is negative in consistent with the negative value of R_H. Similar to the trend of $\rho(T)$, $\alpha(T)$ of Zn-doped samples decrease gradually with the increase of y. For samples with $y > 0.10$, the value of $\alpha(T)$ ranges from -190 μV/K to -280 μV/K at temperatures from 300 K to 600 K. In Fig. 2(c), the power factor PF ($=\alpha^2/\rho$) is presented. For $y = 0.42$, the PF is enhanced in the entire test temperature range and the magnitude spans the range from 11.6 to 15.1 μW/cmK^2. The value is more than 10% higher compared with that of nondoped one.

C. Thermal transport properties and figure of merit

Figure 3 displays the temperature dependence of thermal conductivity $\kappa(T)$ for a selected sample with $y = 0.10$. The value of $\kappa(T = 300\,\text{K})$ is 0.83 W/mK, being a little larger than that of $y = 0$. The low κ in BGS was attributed to the large cage volume and heavier average element mass.[8] Upon heating, $\kappa(T)$ for $y = 0.10$ first decreases slightly and then rapidly increases to 1.21 W/Km at 600 K. The rapid increase in $\kappa(T)$ for $T > 500$ K is attributed to an enhancement of ambipolar thermal conductivity.[21] Compared with the nondoped sample, Zn-doped sample exhibiting lower $\rho(T)$ shows higher $\kappa(T)$ up to 580 K. However, the ambipolar effect appearing above 460 K becomes less pronounced upon Zn doping. For other samples, the data of

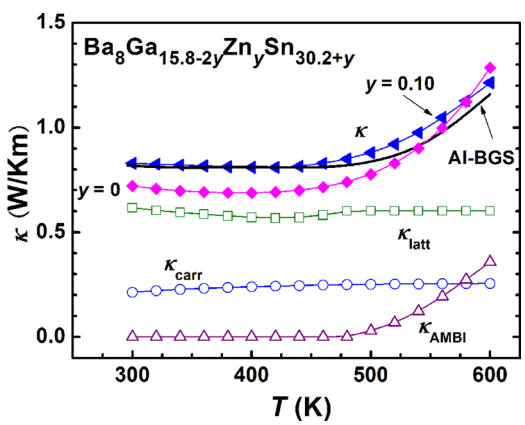

FIG. 3. (Color online) Temperature dependence of thermal conductivity κ for $Ba_8Ga_{15.8-2y}Zn_ySn_{30.2+y}$ ($y = 0$ and 0.10). The κ_{latt}, κ_{carr}, and κ_{AMBI} are the lattice, carrier, and ambipolar contributions for $y = 0.10$ sample, respectively. The data of κ for $Ba_8Ga_{12}Al_4Sn_{30}$ (Al-BGS) were taken from Ref. 14.

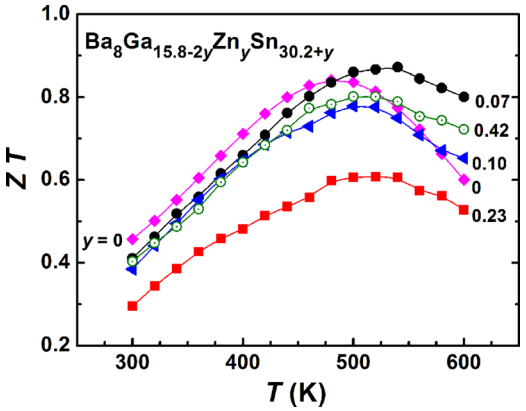

FIG. 4. (Color online) ZT values as a function of temperature for $Ba_8Ga_{15.8-2y}Zn_ySn_{30.2+y}$ ($y = 0 \sim 0.42$).

$\kappa(T)$ could not be collected because the diameter of single crystal was smaller than 6 mm, which size is the minimum requirement for the measurement by the laser-flash method. The total thermal conductivity κ of semiconductors or semimetals with apparent ambipolar thermal conductivity is written as $\kappa = \kappa_{latt} + \kappa_{carr} + \kappa_{AMBI}$, where κ_{latt}, κ_{carr}, and κ_{AMBI} are the lattice, carrier, and ambipolar contributions,[22] respectively. The carrier component can be calculated using the Wiedemann-Franz law as $\kappa_{carr} = LT/\rho$,[23] where the Lorenz number L is 2.45×10^{-8} V^2/K^2 for the fully degenerate semiconductor. The line in Fig. 3 displays the κ value of $Ba_8Ga_{12}Al_4Sn_{30}$ (Al-BGS)[14] with almost equal carrier density, resistivity and κ_{carr} as the sample with x = 0.1. From the similar values of κ, we deduce that the lattice vibration and the ambipolar effect contribute to the total thermal conductivity in a same way for all samples. Moreover, calculations of the effective mass and band gap imply that the band structure remains intact upon Zn doping and carrier density optimization.[12,13] All samples, therefore, should share very similar value of κ_{AMBI} which is mainly determined by the band structure and carrier density. Assuming the κ_{latt} becomes constant above 460 K and κ_{AMBI} can be neglected below 460 K, we can separate the total thermal conductivity for $y = 0.10$ into three terms as shown in Fig. 3. For other samples, κ is calculated by the following equation, $\kappa = \kappa_{latt}$ $(y = 0.10) + \kappa_{carr} + \kappa_{AMBI}$ $(y = 0.10)$.

Based on the measured values of ρ, α, and calculated data of κ, the dimensionless thermoelectric figure of merit $ZT = \alpha^2 T/\rho\kappa$ of $Ba_8Ga_{15.8-2y}Zn_ySn_{30.2+y}$ ($y = 0 \sim 0.42$) samples was calculated and plotted in Fig. 4. The ZT values of the Zn-doped samples are rather low at 300 K, but at elevated temperatures they except for $y = 0.23$ become comparable with that of $y = 0$. Above 500 K, the benefit of Zn doping is clearly manifested itself as the ZT for the sample with $y = 0.42$ reaches 0.87 at 540 K. This value is marginally higher than that of nondoped BGS. However, due to the increase of power factor, the ZT of samples with $y = 0.07$ and 0.42 remains at rather high values above 0.7 near 600 K, which might enhance the overall efficiency of the clathrate BGS in the whole operating temperature range.

IV. CONCLUSION

Single crystals of Zn-substituted type-VIII clathrate $Ba_8Ga_{16}Sn_{30}$ were grown from Sn-flux. The actual composition of the single crystal can be described as $Ba_8Ga_{15.8-2y}Zn_ySn_{30.2+y}$ ($y = 0 \sim 0.54$). The lattice parameter at room temperature increases linearly with y which is a result of the increase of the ratio of Sn/Ga in the cage. The resistivity at 300 K decreases from 5.3 to 3.0 mΩ cm gradually as y goes from 0 to 0.42. The effective mass is essentially constant at $1.2 \sim 1.5m_0$, indicating intact band structure near the conduction band minima upon Zn substitution for Ga. With respect to $y = 0$, substituted samples show higher thermal conductivity up to 580 K, while the ambipolar effect appearing above 460 K becomes less pronounced upon Zn doping. Due to the increase of power factor, the values of ZT for $y = 0.07$ and 0.42 remain at rather high values above 0.7 near 600 K. Thus, the overall efficiency of clathrate $Ba_8Ga_{16}Sn_{30}$ will be enhanced by choosing proper doping elements and levels depending on the application temperature range.

ACKNOWLEDGMENTS

We are grateful to Y. Kono, N. Ohya, and T. Taguchi for thermal diffusivity measurement and Y. Shibata for EPMA performed at Natural Science Center for Basic Research and Development, Hiroshima University. This work was supported by New Energy and Industrial Technology Development Organization (NEDO, Grant No. 09002139-0), and Grant-in-Aid for Scientific Research from MEXT of Japan (Grant Nos. 19051011 and 20102004).

[1]D. M. Rowe, *Handbook of Thermoelectrics: Macro to Nano* (CRC, Boca Raton, FL, 2006).
[2]P. Pichanusakorn and P. Bandaru, Mater. Sci. Eng. R **67**, 19 (2010).
[3]G. A. Slack, in *CRC Handbook of Thermoelectrics*, edited by D. M. Rowe (CRC, Boca Raton, FL 1995).
[4]G. Snyder and E. Toberer, Nat. Mater. **7**, 105 (2008).
[5]K. Koumoto, I. Terasaki, and R. Funahashi, MRS Bull. **31**, 206 (2006).
[6]A.V. Shevelkov and K. Kovnir, in *Zintl Clathrates: In Principles and Recent Developments*, edited by T. F. Fässler (Springer, Heidelberg/Dordrecht/London/New York, 2011).
[7]J. Dong, O. F. Sankey, and C. W. Myles, Phys. Rev. Lett. **86**, 2361 (2001).
[8]M. A. Avila, K. Suekuni, K. Umeo, H. Fukuoka, S. Yamanaka, and T. Takabatake, Phys. Rev. B **74**, 125109 (2006).
[9]H. G. von Schnering, W. Carrillo-Cabrera, R. Kröner, E -M. Peters, and K. Peters, Z. Kristallogr.-New Cryst. Struct. **213**, 679 (1998)
[10]W. Carrillo-Cabera, R. Cardoso. Gil, V.-H. Tran, and Yu. Grin, Z. Kristallogr.-New Cryst. Struct **217**, 181 (2002)
[11]K. A. Kovnir and A. V. Shevelkov, Russ. Chem. Rev. **73**, 923 (2004).
[12]Y. Kono, N. Ohya, T. Taguchi, K. Suekuni, T. Takabatake, S. Yamamoto, and K. Akai, J. Appl. Phys. **107**, 123720 (2010).
[13]Y. Saiga, K. Suekuni, S. Deng, T. Yamamoto, Y. Kono, N. Ohya, and T. Takabatake, J. Alloys Compd. **507**, 1 (2010).
[14]S. Deng, Y. Saiga, K. Suekuni, and T. Takabatake, J. Appl. Phys. **108**, 073705 (2010).
[15]S. Deng, Y. Saiga, K. Kajisa, and T. Takabatake, J. Appl. Phys. **109**, 103704 (2011).
[16]D. Cederkrantz, M. Nygren, and A. Palmqvist, J. Appl. Phys. **108**, 113711 (2010).
[17]D. Huo, T. Sakata, T. Sasakawa, M. A. Avila, M. Tsubota, F. Iga, H. Fukuoka, S. Yamanaka, S. Aoyagi, and T. Takabatake, Phys. Rev. B **71**, 075113 (2005).
[18]M. A. Avila, K. Suekuni, K. Umeo, and T. Takabatake, Physica B **383**, 124 (2006).
[19]M. A. Avila, K. Suekuni, K. Umeo, and T. Takabatake, J. Phys.: Condens. Matter **18**, 1585 (2006).
[20]M. Cutler, J. F. Leavy, and R. L. Fitzpatrick, Phys. Rev. **133**, A1143 (1964).
[21]H. J. Goldsmid, *Introduction to Thermoelectricity* (Springer, Heidelberg, 2010).
[22]V. Jovovic and J. P. Heremans, Phys. Rev. B **77**, 245204 (2008).
[23]G. Chester and A. Thellung, Proc. Phys. Soc. (London) **77**, 1005 (1961).